Research Article

Fuxing Lin*

Study on the performance of nanoparticle-modified PVDF membrane in delaying membrane aging

https://doi.org/10.1515/chem-2024-0124
received May 9, 2024; accepted December 6, 2024

Abstract: With an emphasis on improving the membrane's long-term durability and filtering efficiency, this study examines how well nanoparticle-modified polyvinylidene fluoride (PVDF) membranes perform in postponing membrane aging. The functionalization of PVDF membranes with mesoporous silica nanoparticles (MSNs) to increase their resistance to fouling and degradation makes this study novel. Sol–gel synthesis was used to create MSNs, which were then included in the PVDF membrane matrix. Brunauer–Emmett–Teller surface area analysis, X-ray diffraction, and scanning electron microscopy were used to analyze the structural characteristics of the modified membranes. The findings showed that adding MSNs improved the mechanical strength and permeability of the membrane by increasing its surface area and pore volume. Comparing the modified PVDF membranes to the unmodified membranes, aging tests revealed a slower drop in filtering performance and increased resilience to fouling and chemical degradation. According to these results, MSN-modified PVDF membranes are a promising material for water treatment and other filtering applications since they have a great deal of potential to increase the longevity and effectiveness of filtration systems.

Keywords: PVDF membrane, nanoparticle modification, membrane aging, retardation, oxidative degradation, water treatment

1 Introduction

Polyvinylidene fluoride (PVDF) membranes have been a widely used separation material in the water treatment, biomedical, and energy fields in recent years [1,2]. PVDF membranes are extensively employed in microfiltration, ultrafiltration, and nanofiltration separation processes due to their superior chemical stability, mechanical strength, and resilience to high temperatures. However, PVDF membranes often experience surface aging after extended use, which reduces separation performance and shortens membrane life and has a negative impact on the membrane's application effect and economy [3,4].

Physical damage, biological contamination, and oxidative degradation are the three basic processes of PVDF membrane aging. One of the primary aging processes among them is oxidative degradation [5,6]. During the water treatment process, oxidants, free radicals, and UV light can easily affect the PVDF membrane's surface. This can trigger an oxidative degradation reaction that can lead to various phenomena, including color changes, chemical bond breaks, and pore structure destruction of the membrane materials. Ultimately, these events can impact the membrane's stability and separation performance [7,8]. As a result, one of the key concerns in current research is how to improve the long-term durability of PVDF membranes while postponing their aging.

Researchers have suggested a number of approaches to address the issue of PVDF membrane aging, such as surface modification, material modification, and antioxidant addition [9]. Among these, modification techniques based on nanoparticles have garnered significant interest. The size effect, interfacial effect, and enormous specific surface area of nanoparticles make them particularly advantageous for material modification [10]. PVDF membrane materials that have nanoparticles added to them have better mechanical strength and chemical resistance in addition to having a longer service life and a slower rate of aging [11].

The purpose of this work is to examine how well PVDF membranes treated with nanoparticles slow down membrane aging. Our goal is to provide theoretical and experimental foundations for the applications of nanoparticles and to uncover the mechanism of their influence on PVDF membrane aging through a thorough monitoring and

* **Corresponding author: Fuxing Lin,** School of Resources and Chemical Engineering, Sanming University, Sanming, 365004, Fujian, China, e-mail: 20180105@fjsmu.edu.cn

analysis of the physicochemical properties and chemical composition of both the original and modified membranes. Our goal is to produce effective and stable separation materials for water treatment and other applications, as well as a scientific foundation for optimizing PVDF membrane preparation and application through comparative analysis of changes in membrane performance under various conditions.

2 Materials and tools for experiments

2.1 Materials and reagents for experiments

All chemicals, including tetraethyl orthosilicate (TEOS), cetyltrimethylammonium bromide (CTAB), curcumin, and other reagents, were purchased from recognized suppliers. The instruments used in this study, including the UV–Vis spectrophotometer, Fourier-transform infrared (FTIR) spectrometer, and dynamic light scattering instrument, were sourced from established manufacturers and calibrated according to the standard protocols provided by the manufacturers. Table 1 lists the primary experimental reagents utilized in this investigation [12].

2.2 Experimental instrumentation

Mesoporous silica nanoparticles (MSNs) were synthesized using a sol–gel method. TEOS was used as the silica precursor, with CTAB acting as the template. The mixture was stirred in an aqueous solution, and the pH was adjusted using NaOH. The reaction proceeded at room temperature, and the MSNs were collected by centrifugation, followed by washing and drying. The apparatus used for membrane production is shown in Table 2 [13].

2.3 Experimental procedures for testing free radicals

2.3.1 Method of spectrophotometry for salicylic acid

Salicylic acid spectrophotometry is a straightforward and user-friendly test technique that is one of the most efficient ways to measure antioxidants because of its many advantages, such as low cost and easy availability of salicylic acid, sensitive response, low natural oxidation, and excellent stability. Salicylic acid can be used to absorb the produced hydroxyl radicals (HO−) and convert them into 2,3- and 2,5-dihydroxybenzoic acids. These compounds have a maximum absorption wavelength of 510 nm, and their concentration in sodium hypochlorite solutions can be ascertained using this method. Sodium hypochlorite, which releases active chlorine and active oxygen when applied, is a commonly used low-cost chemical cleaning agent with excellent oxidizing capabilities. This study examined the production of free radicals in sodium hypochlorite solution and assessed the rate at which nanoparticles scavenged hydroxyl radicals (HO−) using a modified salicylic acid spectrophotometric technique in a NaClO system [15].

Table 1: List of the descriptions and experimental reagents

Reagent	Purity	Manufacturer	Notes
Nano-TiO_2	Purity above 99%	Nanjing Xianfeng Nanomaterial Technology Co., Ltd	Particle size 15–25 nm
$MWCNT_S$-COOH	Purity above 99%	Chengdu Organic Chemistry Co., Ltd., Chinese Academy of Sciences	Average length 10–20 nm
PVDF	Pure analytical	Tianjin's Guangfu Fine Chemical Research Institute	—
Polyvinyl pyrrolidone (PVP)	Pure analytical	Tianjin's Guangfu Fine Chemical Research Institute	—
NMP	Pure analytical	Tianjin Bailun Biotechnology Co., Ltd	—
5,5-dimethyl-1-pyrroline-N-oxide (DMPO)	Purity above 97%	Aladdin Chemical Company Ltd	—
Salicylic acid	Analytical pure	Tianyi Chemical Reagent Factory, Tianjin North	—
Anhydrous ethanol	Analytical pure	The chemical reagent technology company Tianjin Fengchuan Co., Ltd	—
$FeSO_4{\cdot}7H_2O$	Analytical pure	The chemical reagent technology company Tianjin Fengchuan Co., Ltd	—
Ferric chloride	Analytical pure	Tianyi Chemical Reagent Factory, Tianjin North	—
Bovine serum albumin	Analytical pure	Beijing Solebao Technology Co., Ltd	—
NaClO	Analytical pure	Yingda Rare Chemical Reagents in Tianjin	—
HCL	Analytical pure	Yingda Rare Chemical Reagents in Tianjin	—
NaOH	Analytical pure	The chemical reagent Tianjin Fengchuan Co., Ltd	—
H_2O	—	Milli-Q^{TM} water	—

Table 2: Instruments for membrane production

Name	Model	Manufacturer
Wet film preparer	—	Modern Environmental Engineering Technology Co., Ltd
Mixer	MYP2011-250	Mei Yingpu Instrument
Digital temperature control electric heating sleeve		Taist instrument
Digital temperature control electric heating sleeve	98-T-C	Taist instrument
Ultrasonic Cleaning Machine	SB-520DTD	Xinzhi Biotechnology Co., Ltd
Electronic balance	ES-1002	DeAnte Sensing Technology Co., Ltd
Electric blast drying oven	DGG-101-3S	Tianyu Experimental Instrument Co., Ltd
Diaphragm pump	EC-204-400A	Delta Electric Technology Co., Ltd

The instruments used for characterization are shown in Table 3 [14].

The following were the precise operation steps: First, a standard curve for the concentration and absorbance of free radicals was established. Subsequently, 2 mL of ethanol, salicylic acid, and water combination were added one at a time into several 25 mL colorimetric tubes. Next, 0, 0.1, 0.2, 0.3, 0.4, 0.5, 0.6, 0.7, 0.8, 0.9, and 1 mL of the ferric chloride standard solution, which had a concentration of 10 mM, were added. Finally, the colorimetric tubes were filled with the necessary volume of deionized water until the total volume of solution reached 15 mL. To make the total volume of solution in the cuvette 15 mL, the appropriate amount of deionized water was added. After the solution was uniformly disseminated by ultrasonic shaking, it was heated for 10–20 min at 37°C in a water bath. The absorbance was measured after the solution was eliminated. After passing through a 0.45 μm filter membrane, the absorbance at 510 nm was measured using a UV spectrophotometer. Next, using the obtained absorbance values to create a standard curve, the number of radicals was ascertained.

Since the components of sodium hypochlorite solution are known to be significantly impacted by its pH, research on the concentration of free radicals generated by NaClO at various pH values will be beneficial for future developments in the chemical cleaning of ultrafiltration membranes. Two milliliters of a mixture of ethanol, salicylic acid, and water used as a trapping agent were introduced to a cuvette along with 1 mL of sodium hypochlorite solution (2,000 ppm) with a pH range of 1–12, 1 mL of ferrous sulfate solution (10 mM), and the appropriate amount of deionized water. The pH of a particular concentration of sodium hypochlorite solution was adjusted to 1, 2, 3, 4, 5, 6, 7, 8, 9, 10, 11, and 13 with acid and alkali solutions, respectively. In order to make the total volume of the solution in the cuvette 15 mL, 1 mL of sodium hypochlorite solution (2,000 ppm, pH = 1–12) was added. Following 10–20 min of ultrasonic shaking, after heating the sodium hypochlorite solution for an extra 10–20 min at 37°C, the absorbance of the solution was measured. Using the standard curve, the absorbance of the sodium hypochlorite solution pH = 1–12 was then obtained as a function of the radical concentration.

In order to test the nanoparticles' capacity to scavenge free radicals, 0.13, 0.27, 0.40, 0.80, 1.80, 3.60, 5.40, 7.20, 9.00, and 10.80 g/L of nano-TiO_2 and MWCNTs-COOH were introduced to each cuvette. After that, the samples' absorbance was calculated using the Axe method, which was previously mentioned. The free radical scavenging rate of the sample is shown in equation (1). Table 4 shows the reagent dosage of the colorimeter.

Table 3: Characterization instruments

Name	Model	Manufacturer
Freeze dryer	SCIENTZ-10N	Xinzhi Biotechnology Co., Ltd
Precision electronic balance	AX224ZH	Ohus Instruments Co., Ltd
pH meter	PB-10	Sedolis Instruments Co., Ltd
Ultra-low-temperature storage box	SW-86L388	Haier Special Electrical Appliances Co., Ltd
UV–vis	DR6000	HACH
Electron spin resonance instrument	JesO-FA200	JEOL
Fourier Transform Infrared spectrometer	Vertex70	Brooke Technology Co., Ltd
Scanning electron microscope	Hitachi S4800	Hitachi Corporation
Fully automatic contact angle measuring instrument	DSA30S	German Kruss Scientific Instrument

$$\text{Clearance } \% = \left(\frac{A_0 - A_X + A_{X0}}{A_0} \right) \times 100\%, \quad (1)$$

where A_X is the sample's absorbance value, A_{X0} is the absorbance value of the blank group without the addition of sodium hypochlorite solution, and A_0 is the control group's absorbance value without the addition of nanoparticles.

2.3.2 Electron spin resonance (ESR) method

By adding a spin-trapping agent to the target of investigation, the principle of ESR is to use the spin-trapping agent to reflect the changes and patterns of the surrounding physical and chemical properties [16]. The use of distinct spin-trapping agents is necessary to counteract different kinds of free radicals, but this approach is costly. This experiment uses a very sensitive DMPO capture agent, whose distinctive spectral lines are immediately identifiable and do not affect the outcome of the experiment. Prior to the experiment, 10% sodium hypochlorite solution was diluted 50 times to create 2,000 ppm of the final solution. The DMPO must be prepared by mixing 250 mg with 11 mL of ultrapure water to make 200 mM of the capture agent. The DMPO is easily deteriorated and must be refrigerated at −20°C with light protection; additionally, it must typically be dozens of times larger than the concentration of the radicals to be effectively captured. A JesO-FA200 electron spin resonator from Japan was used for the experiments, and its frequency and microwave energy were set at 9,000 MHz and 1 mW, respectively.

The experiment involved taking 200 μL of diluted DMPO trap (200 mM) and 100 μL of 10 mM ferrous sulfate solution at the same time, then adding 100 μL of 2,000 ppm sodium hypochlorite solution to the centrifuge tubes while continuously shaking them. In order to prevent interference from impurities, this was followed by filtration through an aqueous filtration membrane with a thickness of 0.22 μm. Finally, three capillary tubes were sampled, their sampling end was sealed with petroleum jelly, and then they were placed in special glass tubes for ESR testing. Free radicals only have a minute to live, so the procedure should be finished in that time. Different kinds of free radicals generated in sodium hypochlorite solutions at various pH values (= 3, 6, 9, 12) were examined using the following experimental setup. Furthermore, 0.01 g of various additives, such as PVP, TiO_2 nanoparticles, and MWCNTs-COOH, were introduced into the centrifuge tubes. The effects of these additions on the kinds of free radicals generated in sodium hypochlorite solutions were examined.

Table 4: Dosage of reagents in colorimetric tubes

Reagent	A_0	A_X	A_{X0}
Ethanol–salicylic acid–water mixture	2	2	2
Ferrous sulfate solution	1	1	1
Additive	0	0.1–1	0–1
Water that has been deionized	10	10–11	10–11
Solution of sodium hypochlorite	1	1	0

3 Methods for preparing membranes and aging membranes

The non imprinted polymer (NIPS) approach was used to prepare PVDF-PVP pristine unmodified membranes, PVDF-PVP/TiO_2 co-modified membranes, and MWCNTs-COOH co-modified membranes [17,18]. The following were the preparation steps.

3.1 Configure the cast film solution

Prepare big beakers, measuring cylinders, dry, clean three-necked flasks, and other equipment. Also, ensure that all of the medications are totally dry. Weigh the necessary solvents, additives, and membrane materials in accordance with formula ratios displayed in Tables 2–5 for PVDF casting solution. Weigh PVDF (36 g), NMP (156 mL), and PVP (8 g) in accordance with the ratio to prepare the PVDF-PVP membrane; weigh nano-TiO_2 (1 g), PVDF (36 g), NMP (156 mL), and PVP (7 g); weigh MWCNTs-COOH (1 g), PVDF (36 g), NMP (156 mL), and PVP (7 g) to prepare the PVDF-PVP/CNT membrane. Batches of the aforementioned substances were added to a flask with three necks. Specifically, in order to prepare the PVDF-PVP/TiO_2 and PVDF-PVP/CNT membranes, the nanoparticles and part of the solvent must be added to a flask with three necks. The

Table 5: PVDF pouring solution ratios

Name	PVDF (wt%)	NMP (wt%)	PVP	NaO-TiO_2	MWCNTs-COOH
PVDF-PVP	16	75	4	0	0
PVDF-PVP/TiO_2	16	75	3.2	0.6	0
PVDF-PVP/CNT	16	75	3.2	0	0.6

nanoparticles must then be uniformly dispersed in the solvent using ultrasound for approximately 20 min, after which the remaining casting solution must be added.

3.2 Heat and stir

To create a homogenous casting solution, the three-necked flask was put in a heating stirrer and mechanically agitated (450 rpm) for over 8 h at a predetermined temperature (70°C).

3.3 Leave to defoam

Once the stirring is stopped, heat the cast film solution further, maintain it at a low temperature, and let it defrost for 12 h, or until the bubbles are observed on the surface of the solution evaporate.

3.4 Scratch the film

Once the film casting solution had reached room temperature, it was defoamed and then placed onto a glass plate with a smooth, dry surface. The film was then scraped evenly and steadily using a wet film preparator (200 µm thick × 100 mm long). Ultimately, a solidification bath (deionized water, 25°C) was rapidly added to the glass plate containing the scraped film.

3.5 Membrane collection and preservation

After scraping the membrane and immersing it in the solidification bath for about 2 min, the PVDF flat membrane, measuring 100 mm by 200 mm and having a thickness of 0.2 mm, can be obtained by withdrawing the membrane. The membrane was put in deionized water to be stored for usage after being categorized and labeled in accordance with various raw material ratios.

To conduct additional research on the impact of varying nanoparticle dosages on the aging of PVDF blend-modified membranes, the blend-modified membranes PVDF-PVP/TiO_2-0.25, PVDF-PVP/CNT-0.25, PVDF-PVP/CNT-0.25, PVDF-PVP/CNT-0.25, and 1 wt% were prepared in accordance with the membrane preparation method in Section 2.3.1. These were prepared in addition to the 0.5 wt% nanoparticle-modified membranes PVDF-PVP/TiO_2-0.5 and PVDF-PVP/CNT-0.5 that were prepared previously. PVP/TiO_2-0.25, PVDF-PVP/TiO_2-1, PVDF-PVP/CNT-0.25, and PVDF-PVP/CNT-1, the amount of nanoparticle additives should be increased to enhance the ultrasonic time. As shown in Figure 1, the processing of PVDF involves more uniform dispersion of nanoparticle additives, which will help to form a uniform size of the membrane structure. Table 6 displays the amount of each component that is cast into the membrane solution. After being labeled, the membranes were left in deionized water for a full day. The membranes were exposed to accelerated aging using NIPS technique after a 24-h period. Additionally, the membranes were treated for 30 days at pH = 9 with sodium hypochlorite. After that, 2,000 ppm of sodium hypochlorite was applied to the membranes.

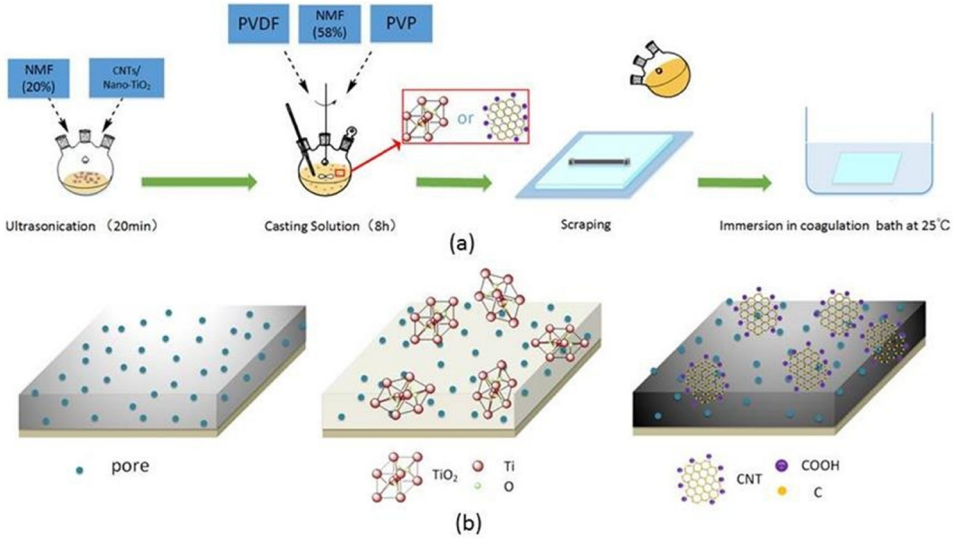

Figure 1: (a) Procedure for preparing PVDF flat membranes and (b) from left to right, PVDF-PVP, PVDF-PVP/TiO_2, and PVDF-PVP/CNT, respectively.

Table 6: Film casting solution ratio with varying doses of nanoparticles

Name	PVDF (wt%)	NMP (wt%)	PVP	NaO-TiO_2	MWCNTs-COOH
PVDF-PVP/TiO_2-0.25	16	75	3.5	0.26	0
PVDF-PVP/TiO_2-0.5	16	75	3.4	0.5	0
PVDF-PVP/TiO_2-1	16	75	3	0.9	0
PVDF-PVP/CNT-0.25	16	75	3.72	1	0.24
PVDF-PVP/CNT-0.5	16	75	3.6	0	0.4
PVDF-PVP/CNT-1	16	75	3	0	1

4 Effect of nanoparticles on the chemical composition of membranes after aging

4.1 Infrared spectral analysis

When viewed in conjunction with the findings of Table 7 and Figure 2(a)'s FTIR infrared spectroscopy analysis, it is evident that each of the three membrane materials made using the NIPS blend-modification approach displays the characteristic features of PVDF spectra. For instance, the CF_2 asymmetric stretching vibration is represented by the peak at 840 cm^{-1}. However, the peak at 1,403 cm^{-1} represents the CH_2 rocking vibration. The peaks of modified PVDF-PVP/TiO_2 and PVDF-PVP/CNT disappeared at 510 cm^{-1}, indicating that nanoparticles caused PVDFs to undergo a phase transition from the α-crystalline phase to the β-crystalline phase. In PVDF-PVP, a noticeable CF_2 bending vibration peak was found at 510 cm^{-1}. It was demonstrated that the β-crystalline phase may greatly enhance the composite membranes' hydrophilicity, thermal stability, and anti-pollution qualities in addition to facilitating the membranes' capacity to separate materials. These findings showed that some of the nano-TiO_2 created cross-links with PVDF, increasing the amount of hydrophilic groups on the membrane's modified surface.

Additionally, a considerable quantity of hydrophilic groups, such as −COOH and −OH, were enriched on the modified membrane surfaces in PVDF-PVP/TiO_2 and PVDF-PVP/CNT, according to the stretching vibration absorption peak that corresponds to the hydroxyl group (−OH), which was seen at 3,380 cm^{-1}. The membrane surfaces of PVDF-PVP/TiO_2 and PVDF-PVP/CNT were more abundant in hydrophilic groups, such as −COOH and −OH, than those of PVDF-PVP. The presence of chemical linkages between the additives and the membrane materials was demonstrated by the C═C backbone vibration that was generated at around 1,580 cm^{-1}. The results showed that nano-TiO_2 and MWCNTs-COOH-modified membranes were successfully prepared by the blending method, and the nanoparticles formed a close connection with the membrane matrix PVDF consisting of chemical bonds.

Using FTIR infrared spectroscopy, functional group alterations brought on by the three membrane materials' accelerated aging effect were further assessed (Figure 2(b)). PVDF underwent a defluorination reaction. A portion of PVP was eliminated from the membrane structure, as evidenced by the decline in the peak of the PVP ketohydroxyl C═O bond at 1,668 cm^{-1}. It was shown that continuous contact of PVP with free radicals led to the degradation of PVP, which in turn had an impact on the membrane

Table 7: Distinctive peaks in the infrared spectra of every material used in membrane materials

Film making materials	Functional group	Frequency of vibrations (cm^{-1})
PVDF (α crystalline phase)	CF_2 bending vibration	600
	CF_2 swinging vibration	1,072
PVDF (β crystalline phase)	CF_2 bending vibration	510
	CF_2 asymmetrical stretching vibration	840
	CF_2 symmetric stretching vibration	876
	C–C skeleton vibration	1,176
PVP	NH_2 bending vibration	746
	NH stretching vibration	1,290
	Ketone carbonyl C═O stretching vibration	1,650–1,760

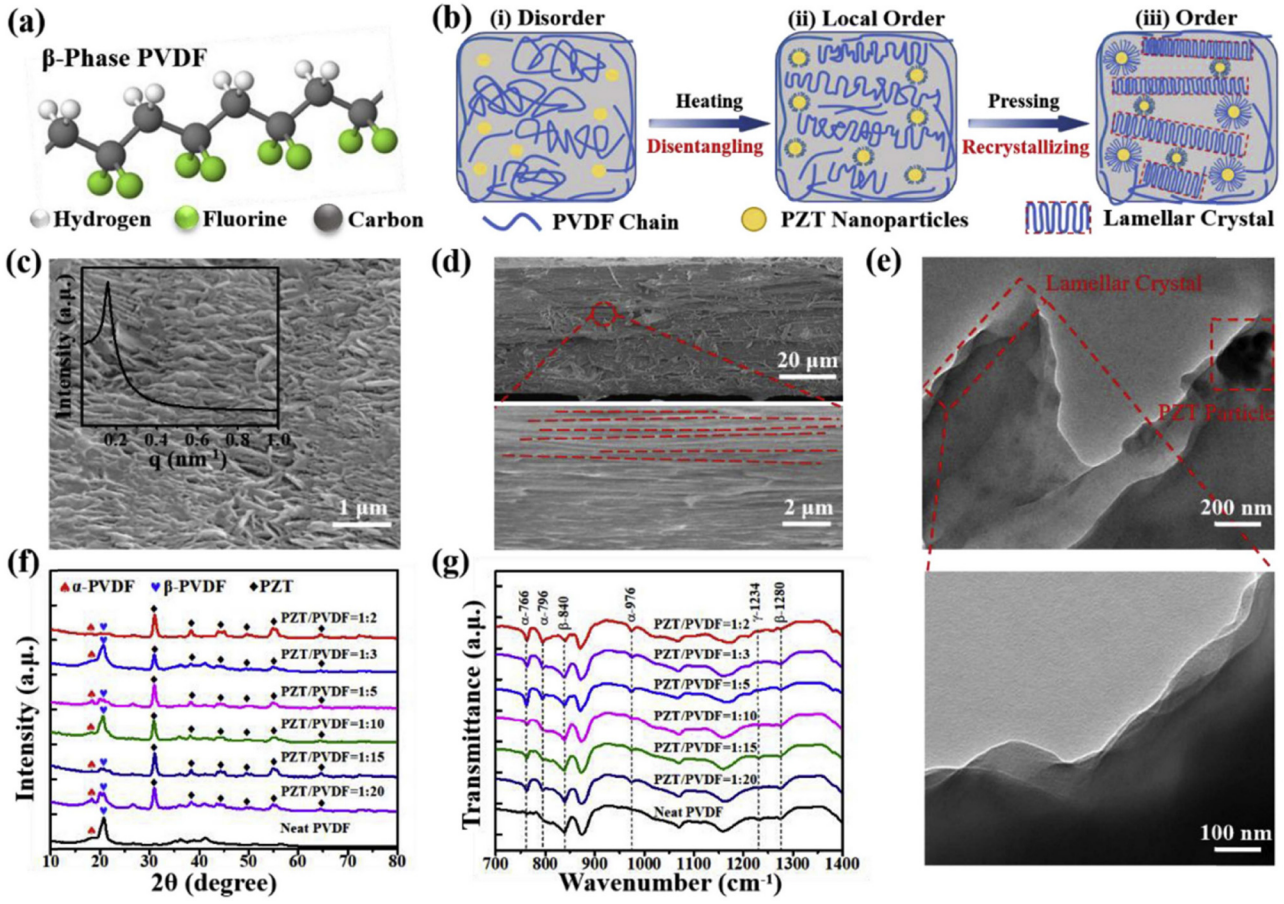

Figure 2: Spectra in the infrared (a) Sans anti-aging medication, (b) following a 30-day anti-aging treatment (c) PVDF-PVP, (d) PVDF-PVP/TiO_2, and (e) PVDF-PVP/CNT. The PVDF-PVP/CNT membrane, in particular, showed a greater degree of chemical stability. Figures 2f and 2g show the density aggregation process and molecular transfer effect of PVDF film, respectively.

properties, such as increased membrane porosity and reduced retention. During chemical aging, the continuous degradation of PVP leads to an increase in surface roughness and a decrease in the hydrophilicity of the membranes. The disappearance of the C═C stretching vibration peak at 1,580 cm^{-1} in PVDF and the C═O fracture of PVP at 1,668 cm^{-1} signal the degradation of the membrane structure and the decrease in mechanical properties. The infrared spectra of the three membrane materials after 30 days of aging are displayed in Figure 2(c–e) following local magnification. It is evident that the characteristic peaks of 1,580 and 1,668 cm^{-1} are decreasing. The infrared characteristic peaks of the PVDF-PVP/TiO_2 and PVDF-PVP/CNT membranes declined less in comparison to the unmodified PVDF-PVP membrane; the PVDF-PVP/CNT membrane, in particular, showed a greater degree of chemical stability. In conclusion, MWCNTs-COOH and nano-TiO_2 may both preferentially bind to the cavities that react to free radicals, preventing PVP degradation and PVDF defluorination reaction while also significantly improving the anti-aging properties of the membranes.

4.2 X-ray spectroscopy

Figure 3(a) and (b) displays the full XPS spectra of the three membrane materials (PVDF-PVP, PVDF-PVP/TiO_2, and PVDF-PVP/CNT) both before and after aging treatment. Conversely, Table 8 displays the elements distribution of the PVDF membranes. The enhanced O1s XPS signals of PVDF-PVP/TiO_2 and the enhanced C1s and O1s XPS signals of PVDF-PVP/CNT, when compared to the XPS spectra of unmodified PVDF-PVP with nanoparticles, show that the PVDF blended membranes with nano-TiO_2 and MWCNTs-COOH have been successfully modified. N, the hallmark element of PVP in PVDF-PVP, nearly vanished after the aging treatment,

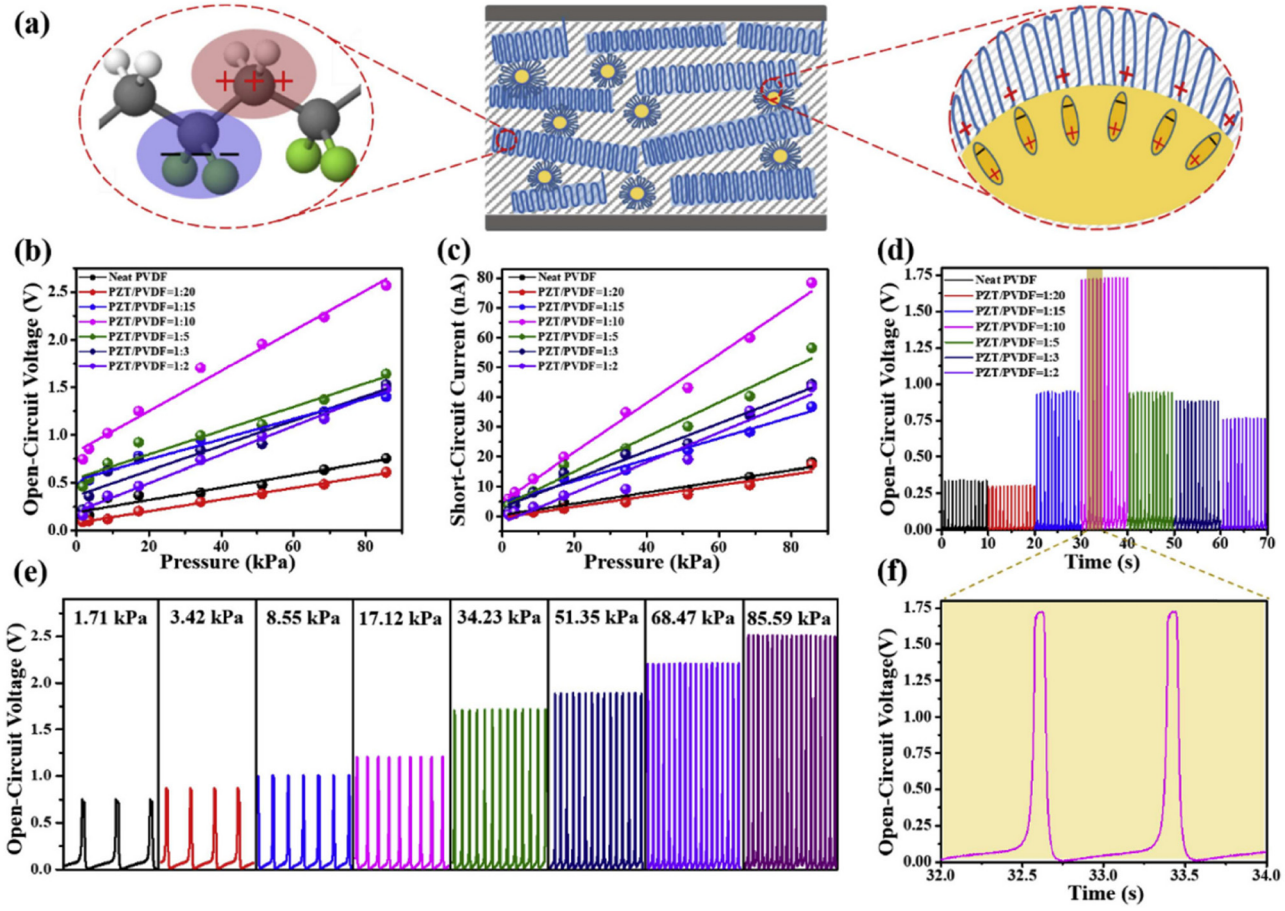

Figure 3: XPS spectra (a) without aging treatment, (b) after 30 days of aging treatment, (c) C1s vs C1s of PVDF-PVP, (d) C1s vs C1s of PVDF-PVP/TiO_2, (e) C1s vs C1s of PVDF-PVP/CNT, and (f) O1s of PVDF-PVP/TiO_2 vs O1s of PVDF-PVP/CNT.

Table 8: PVDF membrane element distribution

Membrane name	C1s	01s	N1s	F1s	Ti_2p
PVDF-PVP	52.71	12.25	4.2	30.82	0
PVDF-PVP-30	58.77	6.22	0	35.05	0
PVDF-PVP-TiO_2	48.55	23.89	1.22	36.56	1.82
PVDF-PVP-TiO_2-30	50.24	9.85	1.22	36.66	1.80
PVDF-PVP/CNT	55.56	14.18	3.62	26.62	0
PVDF-PVP/CNT-30	54.12	9.18	1.13	34.88	0

whereas N1s peaks were still visible in PVDF-PVP/TiO_2 and PVDF-PVP/CNT, indicating that the addition could successfully slow down PVP degradation by sodium hypochlorite. It was determined that some of the TiO_2 nanoparticles were engaged in the reaction by the weakening of the Ti_2p and O1s signals seen in PVDF-PVP/TiO_2. After 30 days of aging treatment, compared to PVDF-PVP, there was no discernible signal weakening of PVDF-PVP/CNT. This could be because the carbon nanotubes and membrane material formed hydrogen bonds, which improves the chemical stability of the membrane.

It was determined that the prominent peak in Figure 3(c)–(e) at 291 eV represented CF_2 and CF bonds. While there was no discernible change in the PVDF-PVP/TiO_2 and PVDF-PVP/CNT, this peak in the PVDF-PVP membrane was considerably attenuated after 30 days of aging treatment. Furthermore, the precipitation of hydrophilic additives, which also contributes to the rise in contact angle and decrease in hydrophilicity after aging, may be the cause of the decrease in the C–O and C–OH peaks at 286.5 eV.

To summarize, the degradation of the PVDF-PVP membrane by sodium hypochlorite was indicated by the considerable decrease in the C–F bond of the unmodified membrane after aging. The C–F linkages in the modified membrane remained strong after aging, indicating that the nanoparticles may be able to stop the aging and membrane

disintegration brought on by sodium hypochlorite. Additionally, some nano-additives were removed from the membrane structure due to the holes and free radicals found in the nanoparticles, and the damage that the free radicals caused to the membrane was lessened by the bursts of radicals.

5 Discussion

This study presents significant advancements in the field of membrane technology through the integration of nanoparticles to prevent aging and enhance performance. The results demonstrate that the incorporation of (specific type of nanoparticles) into the (type of membrane) not only enhances the structural integrity of the membrane but also significantly improves its long-term operational stability. These findings are compared and supported by several reported studies, providing a comprehensive understanding of the innovation and its implications.

Previous studies have explored various types of nanoparticles for membrane enhancement, particularly focusing on improving permeability, selectivity, and mechanical strength. For instance, the study by Calandra et al. [12] utilized different nanoparticles to enhance membrane performance. However, our study distinguishes itself by employing specific nanoparticles, which exhibit superior stability and compatibility with the membrane material, leading to a more pronounced reduction in aging effects.

Our findings show that the specific nanoparticles not only prevent the typical decrease in permeability and selectivity associated with membrane aging but also maintain these properties at an optimal level over extended periods. This is a significant improvement over the results reported by Calandra et al. [12], where the membrane's performance deteriorated after duration due to nanoparticle agglomeration and leaching.

The innovative aspect of this study lies in the precise control over nanoparticle distribution within the membrane matrix, achieved through synthesis method. Unlike previous approaches, where nanoparticles often aggregated, leading to uneven distribution and compromised performance, our method ensures a uniform distribution, enhancing both the mechanical properties and functional longevity of the membrane.

Membrane aging is a critical challenge in long-term applications, and our study provides new insights into mitigating this issue. The adsorption characteristics, permeability, selectivity, and tensile strength of the membranes were thoroughly evaluated, revealing that the incorporation of nanoparticles significantly delays the aging process. These findings are consistent with the theoretical models proposed by Li et al. [18], which suggest that nanoparticles can act as physical barriers, preventing the ingress of aging agents such as oxidants and foulants.

In conclusion, this study significantly advances the field by providing a novel approach to enhancing membrane durability and performance through the strategic incorporation of nanoparticles. The findings are well-supported by reported studies, highlighting the unique contributions and potential applications of this innovation in various industries, including water treatment, gas separation, and beyond.

6 Conclusion

This study has demonstrated the critical role of the type of nanoparticle in significantly enhancing the durability and performance. The key finding is that the incorporation of these nanoparticles not only prevents the common aging processes, such as thermal and chemical degradation, but also maintains the membrane's permeability, selectivity, and tensile strength over an extended operational period.

The innovative approach employed in this study, which ensures a uniform distribution of nanoparticles within the membrane matrix, has proven to be highly effective in addressing the limitations observed in previous studies. This uniform distribution is crucial for preventing nanoparticle agglomeration and leaching, which have been major challenges in earlier attempts to enhance membrane performance. As a result, the membranes developed in this study exhibit a remarkable resistance to aging, maintaining their functional properties far longer than those reported in prior research.

The significance of these findings lies in the potential to revolutionize membrane technology for applications that demand long-term stability and high performance. By effectively mitigating aging, the developed membranes offer a promising solution for industries such as water treatment, gas separation, and other fields where membrane durability is critical. The enhanced lifespan and consistent performance of these membranes can lead to reduced operational costs, lower maintenance requirements, and improved efficiency in various processes.

Acknowledgements: The authors would like to show sincere thanks to those techniques who have contributed to this research.

Funding information: This study was supported by the Natural Science Foundation of Fujian Province (2022J011175);

Natural Science Foundation of Fujian Sanming University National Fund Cultivation Project (PYT2109); Start-up foundation for advanced talents in Sanming University (No. 22YG16).

Author contribution: The author confirms the sole responsibility for the conception of the study, presented results and manuscript preparation.

Conflict of interest: The author declared that there is no conflicts of interest regarding this work.

Ethical approval: The conducted research is not related to either human or animal use.

Data availability statement: The experimental data used to support the findings of this study are available from the corresponding author upon request.

References

[1] Woźniak-Budych M, Zgórzyńska U, Przysiecka Ł, Załęski K, Jarek M, Jancelewicz M, et al. Copper oxide (I) nanoparticle-modified cellulose acetate membranes with enhanced antibacterial and antifouling properties. Environ Res. 2024;252:119068.

[2] Chen J, Wei M, Meng M. Advanced development of molecularly imprinted membranes for selective separation. Molecules. 2023;28(15):5764.

[3] Zhang H, Lin X, Cao X, Wang Y, Wang J, Zhao Y. Developing natural polymers for skin wound healing. Bioact Mater. 2024;33:355–76.

[4] Xiong J, Liu X, Xia P, Guo X, Lu S, Lei H, et al. Modified separators boost polysulfides adsorption-catalysis in lithium-sulfur batteries from Ni@ Co hetero-nanocrystals into CNT-porous carbon dual frameworks. J Colloid Interface Sci. 2023;652:1417–26.

[5] Balsamo JM, Zhou K, Kammarchedu V, Ebrahimi A, Bess EN. Mechanistic insight into intestinal α-synuclein aggregation in Parkinson's disease using a laser-printed electrochemical sensor. ACS Chem Neurosci. 2024;15(14):2623–32.

[6] Yin J, Reddy VS, Chinnappan A, Ramakrishna S, Xu L. Electrospun micro/nanofiber with various structures and functions for wearable physical sensors. Polym Rev. 2023;63(3):715–62.

[7] Kumar R, Ahmed M, Bhadrachari G, Al-Missri A, Thomas JP. The effect of chemistry of nanoparticle modifier groups on the PVDF membranes for membrane distillation. Chem Eng Res Des. 2020;164:1–10.

[8] Mahdavi H, Rahimi A, Alam LA. Preparation, characterization and performance study of modified PVDF-based membranes containing palladium nanoparticle-modified graphene hierarchical nanostructures: as a new catalytic nanocomposite membrane. Polym Bull. 2017;74:3557–77.

[9] Satthiyaraju M, Ramesh T. Nanomechanical, mechanical responses and characterization of piezoelectric nanoparticle-modified electrospun PVDF nanofibrous films. Arab J Sci Eng. 2019;44:5697–709.

[10] Kamarudin D, Awanis Hashim N, Ong BH, Kakihana Y, Higa M, Matsuyama H. Multiple effect of thermal treatment approach on PVDF membranes: Permeability enhancement and silver nanoparticles immobilization. J Environ Chem Eng. 2021;9(4):105769.

[11] Ahmad AY, Tiwari A, Nayeem MA, Biswal BK, Satapathy DP, Kulshreshtha K, et al. Artificial intelligence perspective framework of the smart finance and accounting management model. Int J Intell Syst Appl Eng. 2024;12(4s):586–94.

[12] Calandra D, Secinaro S, Massaro M, Dal Mas F, Bagnoli C. The link between sustainable business models and Blockchain: A multiple case study approach. Bus Strategy Environ. 2023;32(4):1403–17.

[13] Tagde P, Tagde S, Bhattacharya T, Tagde P, Chopra H, Akter R, et al. Blockchain and artificial intelligence technology in e-Health. Environ Sci Pollut Res. 2021;28:52810–31.

[14] Luo X, Zhang C, Bai L. A fixed clustering protocol based on random relay strategy for EHWSN. Digital Commun Netw. 2023;9(1):90–100.

[15] Andronie M, Iatagan M, Uţă C, Hurloiu I, Dijmărescu A, Dijmărescu I. Big data management algorithms in artificial Internet of Things-based fintech. Oecon Copernic. 2023;14(3):769–93.

[16] Zhou H, Sun G, Fu S, Wang L, Hu J, Gao Y. Internet financial fraud detection based on a distributed big data approach with node2vec. IEEE Access. 2021;9:43378–86.

[17] Ugochukwu CE, Ofodile OC, Okoye CC, Akinrinola O. Sustainable smart cities: the role of fintech in promoting environmental sustainability. Eng Sci Technol J. 2024;5(3):821–35.

[18] Li S, Zhao X, Zhang H. Aging retardation strategy of PVDF membranes: evaluation of free radical scavenging effect of nano-particles. New J Chem. 2021;45(13):6108–19.